Title	A flicker-free electrolytic capacitor-less AC-DC LED driver
Author(s)	Wang, S; Ruan, XB; Yao, K; Tan, SC; Yang, Y; Ye, ZH
Citation	IEEE Transactions on Power Electronics , 2012, v. 27 n. 11, p. 4540-4548
Issued Date	2012
URL	http://hdl.handle.net/10722/196283
Rights	IEEE Transactions on Power Electronics . Copyright © Institute of Electrical and Electronics Engineers.

A Flicker-Free Electrolytic Capacitor-Less AC–DC LED Driver

Shu Wang, Xinbo Ruan, *Senior Member, IEEE*, Kai Yao, Siew-Chong Tan, *Senior Member, IEEE*, Yang Yang, and Zhihong Ye

***Abstract*—The electrolytic capacitor is the key component that limits the operating lifetime of LED drivers. If an ac–dc LED driver with power factor correction (PFC) control is allowed to output a pulsating current for driving the LEDs, the electrolytic capacitor will no longer be required. However, this pulsating current will introduce light flicker that varies at twice the power line frequency. In this paper, a configuration of flicker-free electrolytic capacitor-less single-phase ac–dc driver for LED lighting is proposed. The configuration comprises an electrolytic capacitor-less PFC converter and a bidirectional converter, which serves to absorb the ac component of the pulsating current of the PFC converter, leaving only a dc component to drive the LEDs. The output filter capacitor of the bidirectional converter is intentionally designed to have a large voltage ripple, thus its capacitance can be greatly reduced. Consequently, film capacitors can be used instead of electrolytic capacitors, leading to the realization of a flicker-free ac–dc LED driver that has a long lifetime. The proposed solution is generally applicable to all single-phase PFC converters. A prototype with 48-V, 0.7-A output is constructed and tested. Experimental results are presented to verify the effectiveness of the flick-free electrolytic capacitor-less ac–dc LED driver.**

***Index Terms*—Driver, electrolytic capacitor, flicker, light-emitting diode, power factor correction (PFC).**

I. Introduction

LIGHTING is an important aspect of energy consumption. Currently, it consumes 25% of the world's total electric energy production [1]. Naturally, the innovation for green energy-saving lighting has become an important pursuit throughout the world. New light sources should be highly efficient, energy conserving, pollution free, and be able to simulate natural lights [2]. Light-emitting diode (LED) has all the properties of the aforementioned. It has been rapidly developed over the last few years and is gradually becoming a market leading product in some applications, e.g., in mobile products and backlighting of LCD panels [3], [4]. Currently, the applications of LED lighting are mainly concentrated in two aspects. One aspect is for low-brightness illumination, for example, the screen backlighting of notebook computers and mobile phones, and the other is for high-brightness illumination such as general lighting, vehicle lighting, and backlighting of large television panels [5], [6]. The efficiency of conventional LED drivers involving resistor-based current limiters, linear regulators, and charge pumps is very low [7], [8]. Switching power supplies can achieve a high efficiency, high power density, and high control accuracy, which make them ideal candidates as high-power LED drivers [9].

For single-phase LED drivers that utilize an ac input source, power factor correction (PFC) control must be imposed in the driver to achieve a high power factor to meet relevant harmonic standards, e.g., IEC61000-3-2 [10]. In the case of unity power factor, a pulsating power (since the input current is enforced to be varying sinusoidally in phase with the input voltage) will be seen at the input side of the driver, while the output power is typically made constant to drive the LEDs. To balance out the instantaneous power difference between the pulsating input and the constant output, a storage capacitor with large capacitance is required, regardless if the LED driver adopted is of cascaded structure or single-stage structure. Typically, for storage capacitors with such a large capacitance, electrolytic capacitors will be used. The lifetime of an electrolytic capacitor is about 5 000 h [11]. On the other hand, the estimated useful lifetime of LEDs is about 50 000 h [12]. It is general expectation that LED drivers should have a life expectancy close to the lifetime of LEDs. For stand-alone LED drivers, the electrolytic capacitor is found to have the highest failure rate among all components, which makes it the main component limiting the lifetime of the LED driver [13]. Additionally, the use of electrolytic capacitor is also a hindrance toward achieving a high overall power density design of the driver.

In order to extend the expected lifetime of LED drivers, the electrolytic capacitor should be removed from the circuits. One approach of achieving this is through a new driver topology, which uses magnetic energy storage instead of electrolytic-capacitor-based storage [14], [15]. While such a possibility has been demonstrated, it was found that such an approach leads to the tradeoff of a significant increase in the size and weight

Manuscript received April 28, 2011; revised September 28, 2011 and December 8, 2011; accepted December 9, 2011. Date of current version June 20, 2012. This work was supported by Lite-On Technology Corp. Recommended for publication by Associate Editor B. Lehman.

S. Wang and K. Yao were with the Aero-Power Sci-Tech Center, College of Automation Engineering, Nanjing University of Aeronautics and Astronautics, Nanjing 210016, China, when this work was conducted (e-mail: wangshu@nuaa.edu.cn; yaokai@nuaa.edu.cn).

X. Ruan is with the College of Automation Engineering, Nanjing University of Aeronautics and Astronautics, Nanjing 210016, China, and also with the Key State Laboratory of Advanced Electromagnetic Engineering and Technology, Huazhong University of Science and Technology, Wuhan 430074, China (e-mail: ruanxb@nuaa.edu.cn).

S. C. Tan is with the Department of Electronic and Information Engineering, The Hong Kong Polytechnic University, Kowloon, Hong Kong (e-mail: ensctan@polyu.edu.hk).

Y. Yang is with the College of Automation Engineering, Nanjing University of Aeronautics and Astronautics, Nanjing 210016, China (e-mail: zero3eddy@126.com).

Z. Ye is with Power SBG ATD-NJ R&D Center, Lite-On Technology Corp., Nanjing 210019, China (e-mail: Sam.Ye@liteon.com).

Color versions of one or more of the figures in this paper are available online at http://ieeexplore.ieee.org.

Digital Object Identifier 10.1109/TPEL.2011.2180026

of the driver. Another approach of eliminating electrolytic capacitor is through the alleviation of the pulsating component of the input power by sacrificing the input power factor [15]–[18]. The basis of these methods is to intentionally distort the input current such that there is little low-frequency power-ripple component being generated at the input, and hence, there will be little low-frequency ripple reflected at the output voltage. Consequently, the required storage capacitance can be reduced to the extent that long-lifetime capacitors such as film capacitors or ceramic capacitors can be used instead of electrolytic capacitors. The third approach is through the insertion of an active filter to isolate the energy storage capacitor from the input and output terminals of the driver. This will allow the presence of a larger capacitor voltage ripple (while maintaining a fairly constant output voltage at the driver), which means that the required capacitance can be reduced and be replaced by nonelectrolytic capacitors [19]–[23]. However, the drawbacks of these methods include having an overall lower efficiency, increased circuit complexity, and a higher cost. The three approaches mentioned previously are applicable to LED drivers which drive the LEDs using a constant current.

Apart from the use of constant current, pulsating current can also be used to drive LEDs. Based on the experimental investigation reported in [24], within the linear operating range of the LED's flux-versus-current characteristic, the average output flux is approximately proportional to the average value of the driving current and is independent of the frequency of the driving current. What this means is that the ac variation of the current will have no effect on the average illumination generated by the LED. Building on this principle, a type of electrolytic capacitor-less single-stage LED driver is proposed in [25]. The proposed solution allows the actualization of an LED driver that concurrently achieves unity power factor and a potentially longer lifetime as it contains no electrolytic capacitor. However, the output current of this proposed electrolytic capacitor-less LED driver is pulsating with a large ac second-harmonic ripple component that is varying at twice the power line frequency (hereon known as second-harmonic ripple). When passed into the LED, the pulsating current is directly converted into pulsating light of the same frequency. As the frequency of this pulsating light is higher than that of the human visual persistence, the human minds will not be consciously aware of the light flicker. However, in environments where light flickers, the human visual system has to constantly adjust itself to maintain the clarity of the images at the retina. Prolonged activities will severely strain the human eyes and causes great fatigue to the individuals working in such environments [26]–[28]. Therefore, the use of such electrolytic capacitor-less LED drivers, which produce pulsating current to drive the LEDs, may not be suitable for many applications.

In view of this, the objective of this paper is to propose a flicker-free electrolytic capacitor-less single-phase ac-dc LED driver, which converts the ac power source into a constant direct current for driving high-brightness LEDs, e.g., in general illumination applications, etc. Since the proposed LED driver contains no electrolytic capacitor, it potentially has a much longer lifetime than conventional LED drivers. Note that the proposed driver adopts the concept of active filter, which has been previously applied for alleviating harmonics in power electronics systems [19]–[23]. Here, the idea of alleviating the second-harmonic ripple in LED systems using active filter is demonstrated using a bidirectional buck/boost converter. The focus of this paper is the coverage of the theoretical work and the provision of practical guidelines in designing such a filter, both the converter and its control, which were missing from the literature.

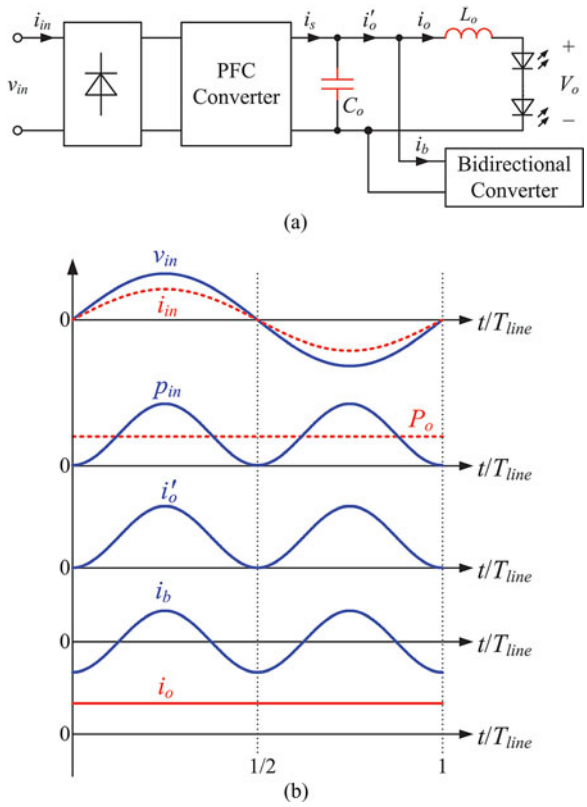

Fig. 1. Flicker-free electrolytic capacitor-less ac–dc LED driver. (a) Schematic diagram. (b) Key waveforms.

In Section II, the concept of the flicker-free electrolytic capacitor-less ac–dc driver is presented. In Section III, the topology and control of the flicker-free electrolytic capacitor-less ac–dc driver are discussed. In Section IV, the relationship between the voltage ripple and the output filter capacitance of the bidirectional buck/boost converter is discussed. The experimental results of a 48-V, 0.7-A output prototype are presented in Section V. This is followed by the conclusions in Section VI.

II. Concept of Flicker-Free Electrolytic Capacitor-Less AC–DC Driver for LED Lighting

Fig. 1(a) shows the schematic diagram of the proposed flicker-free electrolytic capacitor-less ac–dc LED driver. It comprises a PFC converter, a bidirectional converter, a filter capacitor C_o, and a filter inductor L_o. The filter inductor L_o is connected in series with the LED string, and it acts as a low-pass filter in preventing the harmonics at the switching frequency from flowing through LEDs. The filter capacitor C_o provides a low impedance path for the switching-frequency harmonic current ripples of i_s

and i_b to flow through. It must be emphasized that the function of the filter capacitor C_o is different from the conventional storage capacitor as it filters only the high-frequency harmonic ripples, and not the second-harmonic ripple. Therefore, C_o is very small, which offers the possibility of adopting film capacitors or ceramic capacitors instead of electrolytic capacitors. The absence of electrolytic capacitor will significantly increase the lifetime of the PFC converter. Fig. 1(b) shows the key waveforms of the flicker-free electrolytic capacitor-less ac–dc LED driver when the input power factor is unity.

The input voltage is defined as

$$v_{\rm in}(t) = V_m \sin \omega t \tag{1}$$

where V_m is the amplitude of the input voltage and ω is the angular frequency of the input voltage. Here, $\omega = 2\pi/T_{\rm line}$, where $T_{\rm line}$ is the line period of the input voltage.

When unity power factor is achieved, the input current is a sinusoidal waveform that is in phase with $v_{\rm in}$, i.e.,

$$i_{\rm in}(t) = I_m \sin \omega t \tag{2}$$

where I_m is the amplitude of the input current.

From (1) and (2), the instantaneous input power can be derived as

$$p_{\rm in}(t) = v_{\rm in}(t) i_{\rm in}(t) = V_m I_m \sin^2 \omega t = \frac{V_m I_m (1 - \cos 2\omega t)}{2}$$
$$= P_{\rm in}(1 - \cos 2\omega t) \tag{3}$$

where $P_{\rm in} = V_m I_m/2$ is a constant value representing the amplitude of the instantaneous input power.

In the proposed configuration, the output voltage V_o that is applied across the LEDs is a constant dc voltage. Since the current flowing through the filter inductance L_o is dc and contains no ac variation, the voltage across L_o is nearly zero, comprising only a small negligible dc value equivalent to the multiplication of the current and the dc resistance of the inductor. Thus, the voltage in C_o is almost equivalent to V_o.

Assuming that the converter is ideal with no power loss, and that the capacitor C_o is somehow incapable of energy storage, the instantaneous output power of the converter will be equivalent to the instantaneous input power. With this assumption, the current i'_o will be

$$i'_o(t) = \frac{p_o}{V_o} = \frac{P_{\rm in}}{V_o}(1 - \cos 2\omega t). \tag{4}$$

From (4), it is obvious that i'_o contains an ac second-harmonic ripple current that varies sinusoidally at twice the line frequency. If i'_o is allowed to directly drive the LEDs, the generated light from the LED will contain flicker at twice the line frequency. However, in the proposed configuration, the bidirectional converter provides the current flow path for the second-harmonic ripple. To achieve this, i_b is made equal to the second-harmonic ripple component of i'_o, i.e.,

$$i_b(t) = -\frac{P_{\rm in}}{V_o} \cos 2\omega t. \tag{5}$$

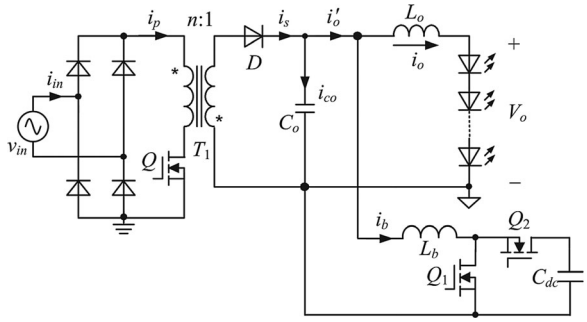

Fig. 2. Circuit topology of the flicker-free electrolytic capacitor-less ac–dc LED driver.

Therefore, the driving current i_o will be

$$i_o(t) = i'_o(t) - i_b(t) = \frac{P_{\rm in}}{V_o}. \tag{6}$$

From (6), it can be seen that the driving current i_o is purely dc, indicating that there will be no flicker from the generated light.

III. Topology and Control of Flicker-Free Electrolytic Capacitor-Less AC–DC LED Driver

A. Topology of the Flicker-Free Electrolytic Capacitor-Less AC–DC LED Driver

The PFC converter illustrated in Fig. 1(a) can be of any converter topology as determined by the required application based on the necessary output voltage or output power, etc. In the case of general consumer or industrial lighting where both the output power and voltage of the LED driver are very low, a flyback converter may be adopted as the PFC converter. In this study, the flyback converter is designed to operate in discontinuous current mode (DCM) so that the switching frequency is constant, which is helpful in the design of the transformer and also that the reverse recovery of the secondary diode D can be avoided. Also, here, the bidirectional buck/boost converter is chosen as the active filter for its simplicity. A topological overview of the proposed flicker-free electrolytic capacitor-less ac–dc LED driver made up of the PFC flyback converter and the bidirectional buck/boost converter is shown in Fig. 2.

B. PFC Flyback Converter

The application of PFC flyback converter in LED drivers has been reported and discussed in detail in [25]. Here, we briefly reiterate its operating principle to allow us to better explain our proposed LED driver.

When a flyback converter operates in DCM, the peak and average values of the primary current i_p in a switching cycle are, respectively

$$i_{p\_\rm pk} = \frac{V_m \left|\sin \omega t\right| D_y}{L_p f_s} \tag{7}$$

$$i_{p\_\rm av} = \frac{1}{2} i_{p\_\rm pk} D_y = \frac{V_m \left|\sin \omega t\right| D_y^2}{2 L_p f_s} \tag{8}$$

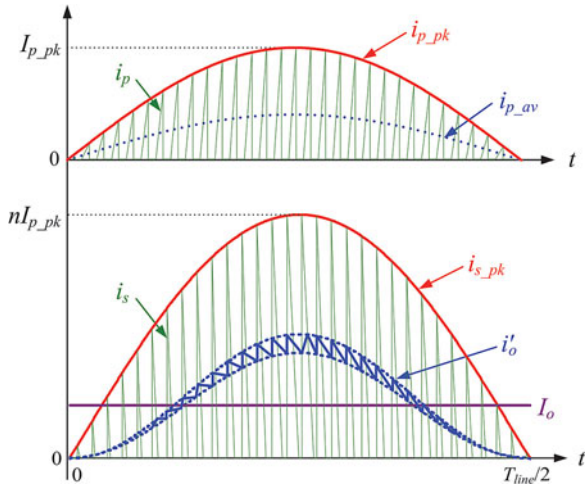

Fig. 3. Waveforms of primary current, secondary current, and output current of the PFC flyback converter.

where D_y is the duty cycle of switch Q, f_s is the switching frequency, and L_p is the primary inductance of the transformer.

It can be seen from (8) that if D_y and f_s are kept constant in a half-line cycle, the input current will be proportional to the input voltage, thereby automatically achieving unity power factor.

Next, the peak value of the secondary current is

$$i_{s\_\mathrm{pk}} = n i_{p\_\mathrm{pk}} = \frac{nV_m \left|\sin \omega t\right| D_y}{L_p f_s} \tag{9}$$

where n is the turns ratio of the primary to secondary windings of the transformer.

From (9) and the relationship of the primary and secondary inductances in terms of the turns ratio, i.e., $L_p/L_s = n^2$, the corresponding duty cycle of the reset time for the secondary current to fall to zero is

$$D_r = \frac{L_s i_{s\_\mathrm{pk}}}{V_o T_s} = \frac{V_m \left|\sin \omega t\right| D_y}{nV_o} \tag{10}$$

where L_s is the secondary inductance of the transformer.

From (9) and (10), the average value of the secondary current in a switching cycle can be expressed as

$$i_{s\_\mathrm{av}} = \frac{1}{2} i_{s\_\mathrm{pk}} D_r = \frac{V_m^2 D_y^2 \sin^2 \omega t}{2V_o L_p f_s} = \frac{V_m^2 D_y^2}{4V_o L_p f_s} \left(1 - \cos 2\omega t\right). \tag{11}$$

The waveforms of the primary and secondary currents are depicted in Fig. 3. It can be seen that the secondary current has a large ripple, and it contains large harmonics at the switching frequency. The presence of L_o and C_o form the output filter, which remove most of the high-frequency harmonic ripples in the secondary current, leaving only the dc current, the second-harmonic ripple, and minimal high-frequency ripples in i'_o.

As L_o and C_o have little effect on the second-harmonic ripple, the average value of i'_o is equal to the average value of the secondary current, i.e.,

$$i'_o = i_{s\_\mathrm{av}} = \frac{V_m^2 D_y^2}{4V_o L_p f_s} \left(1 - \cos 2\omega t\right). \tag{12}$$

The average value of output current over a half-line cycle can be derived as

$$I_o = \frac{2}{T_{\mathrm{line}}} \int_0^{T_{\mathrm{line}}/2} i'_o dt = \frac{V_m^2 D_y^2}{4V_o L_p f_s}. \tag{13}$$

The input power is

$$P_{\mathrm{in}} = \frac{2}{T_{\mathrm{line}}} \int_0^{T_{\mathrm{line}}/2} \left(V_m \left|\sin \omega t\right| i_{p\_\mathrm{av}}\right) dt. \tag{14}$$

Next, the substitution of (8) into (14) yields

$$P_{\mathrm{in}} = \frac{V_m^2 D_y^2}{4L_p f_s}. \tag{15}$$

Thus, the duty cycle with respect to the input power can be expressed as

$$D_y = \frac{2}{V_m} \sqrt{P_{\mathrm{in}} L_p f_s}. \tag{16}$$

The substitution of (16) into (7) and (9), respectively, yields

$$i_{p\_\mathrm{pk}} = 2\sqrt{\frac{P_{\mathrm{in}}}{L_p f_s}} \left|\sin \omega t\right| \tag{17}$$

$$i_{s\_\mathrm{pk}} = 2n\sqrt{\frac{P_{\mathrm{in}}}{L_p f_s}} \left|\sin \omega t\right|. \tag{18}$$

It can be obtained from (17) and (18) that when the input power is constant and that efficiency is 100%, the peak values of the primary and secondary currents of the flyback converter will be constant irrespective of the input voltage.

As previously mentioned, within the linear operating range of the LED's flux-versus-current characteristic, the average output flux of the LED is approximately proportional to the average value of the driving current. Here, the average value of the driving current is taken as the control variable to regulate the output flux of the LEDs. The schematic diagram of the controller for the PFC flyback converter is shown in the top portion of Fig. 4. I_{o_ref} is the reference current and i_o is the feedback signal. However, i_o is a dc current, which cannot be sensed through galvanic isolation. From Fig. 2, it can be seen that the average value of the secondary current i_s is equal to the average output current, and that i_s is a current pulsating at switching frequency. Therefore, by sensing i_s with a current transformer circuit consisting of T_2, D_{ct}, and R_{ct}, and, then, filtering the sensed current signal using the filter comprising R_{f1} and C_{f1}, the desired feedback signal can be obtained.

The sensed current signal and current reference are sent to the error amplifier E/A1, and the output signal of the error amplifier is compared with the sawtooth carrier signal. The output signal of the comparator is sent to pin "R" of the RS flip-flop, to generate the driving signal of switch Q.

C. Bidirectional Buck/Boost Converter

To produce a pure dc current for driving the LEDs, the input current i_b of the bidirectional converter must be equal to the second-harmonic ripple of i'_o. The schematic diagram of the controller for the bidirectional buck/boost converter is shown in

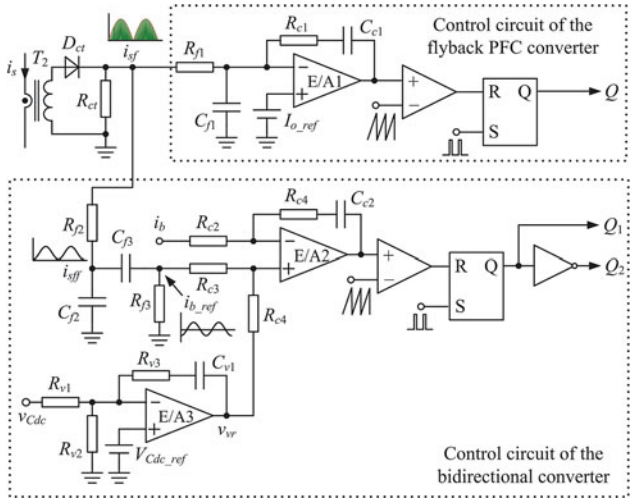

Fig. 4. Control schematic diagram of flicker-free electrolytic capacitor-less ac–dc LED driver.

the bottom portion of Fig. 4. The sensed current, $i_{\rm sf}$, is filtered by R_{f2} and C_{f2} to produce $i_{\rm sff}$. Information on the second-harmonic ripple is then extracted from $i_{\rm sff}$ by the filter comprising C_{f3} and R_{f3}.

For proper operation of the bidirectional converter, the voltage $v_{C\,\rm dc}$ of the capacitor $C_{\rm dc}$ must be set higher than the voltage of C_o. A closed-loop must be included in the controller to enforce this. The voltage of $C_{\rm dc}$ is sensed and compared with the voltage reference $V_{C\,\rm dc\_ref}$, and the amplified error signal v_{vr} is obtained. The sum of $i_{b\_\rm ref}$ and v_{vr} with the weighted resistors R_{c3} and R_{c4}, respectively, is used as the current reference of i_b. The output signal of the error amplifier E/A2 is compared with the sawtooth carrier, and the output signal of the comparator is sent to the RS flip-flop. The signal from pin "Q" is the drive signal of switch Q_1. The drive signal of Q_2 is the inverse of Q_1.

IV. Design of the Bidirectional Converter

The design of the PFC flyback converter with the filtering inductor L_o and capacitor C_o can be found in [25]. In this paper, only the design of the bidirectional converter will be discussed. Note that the bidirectional converter and design procedure discussed here is general and applicable to all PFC converters, and is not limited to the PFC flyback converter.

A. Output Filter Capacitor

The inductor current of the bidirectional converter, i.e., i_b, is controlled to be equal to the second-harmonic ripple of i'_o. From (5), we have

$$i_b = -I_o \cos 2\omega t \tag{19}$$

where $I_o = P_{\rm in}/V_o = P_o/V_o$. Then, the instantaneous input power of the bidirectional converter is

$$p_{bb}(t) = V_{Co} i_b = V_o i_b = -V_o I_o \cos 2\omega t = -P_o \cos 2\omega t \tag{20}$$

where V_{Co} is approximately equal to V_o.

The waveforms of the instantaneous input power p_{bb}, inductor current i_b, and output filter capacitor voltage $v_{C\,\rm dc}$ of the buck/boost converter are depicted in Fig. 5. It can be seen that $C_{\rm dc}$ is charging from time $T_{\rm line}/8$ to $3T_{\rm line}/8$ with $v_{C\,\rm dc}$ increasing, and discharging from time $3T_{\rm line}/8$ to $5T_{\rm line}/8$ with $v_{C\,\rm dc}$ decreasing. Consequently, the minimum and maximum values of $v_{C\,\rm dc}$ occur, respectively, at $T_{\rm line}/8$ and $3T_{\rm line}/8$.

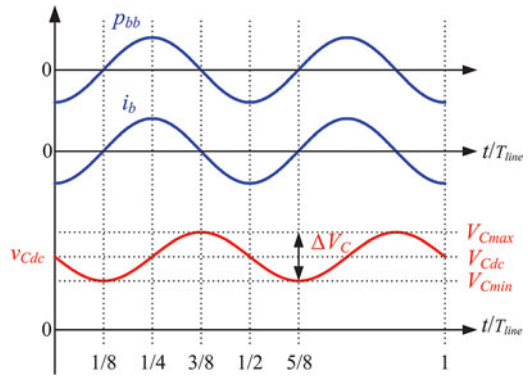

Fig. 5. Waveforms of instantaneous input power, inductor current, and output filter capacitor voltage of the buck/boost converter.

The energy charging $C_{\rm dc}$ from $T_{\rm line}/8$ to $3T_{\rm line}/8$ is

$$\Delta E_{C\,\rm dc}(t) = \int_{T_{\rm line}/8}^{t} p_{bb}(t)dt = \int_{T_{\rm line}/8}^{t} (-P_o \cos 2\omega t)dt = \frac{P_o}{\omega} \sin^2\left(\omega t - \frac{\pi}{4}\right). \tag{21}$$

$\Delta E_{C\,\rm dc}$ can also be expressed as

$$\Delta E_{C\,\rm dc}(t) = \frac{1}{2} C_{\rm dc} v_{C\,\rm dc}^2(t) - \frac{1}{2} C_{\rm dc} V_{C\,\rm min}^2. \tag{22}$$

Substitution of (22) into (21) leads to

$$\frac{1}{2} C_{\rm dc} v_{C\,\rm dc}^2(t) - \frac{1}{2} C_{\rm dc} V_{C\,\rm min}^2 = \frac{P_o}{\omega} \sin^2\left(\omega t - \frac{\pi}{4}\right) \tag{23}$$

where $V_{C\,\rm min}$ is the minimum voltage of the capacitor $C_{\rm dc}$.

From (23), we have

$$v_{C\,\rm dc}(t) = \sqrt{\frac{2P_o \sin^2(\omega t - (\pi/4))}{\omega C_{\rm dc}} + V_{C\,\rm min}^2}. \tag{24}$$

By the substitution of $t = 3T_{\rm line}/8$ into (24), the maximum voltage of the capacitor $C_{\rm dc}$ can be derived as

$$V_{C\,\rm max} = \sqrt{\frac{2P_o}{\omega C_{\rm dc}} + V_{C\,\rm min}^2}. \tag{25}$$

The average voltage of $C_{\rm dc}$ can be approximated as

$$V_{C\,\rm dc} = \frac{V_{C\,\rm min} + V_{C\,\rm max}}{2} = \frac{V_{C\,\rm min} + \sqrt{(2P_o/\omega C_{\rm dc}) + V_{C\,\rm min}^2}}{2}. \tag{26}$$

To ensure the proper operation of the bidirectional converter, the instantaneous voltage of $C_{\rm dc}$ must always be higher than the input voltage of the converter, i.e.,

$$v_{C\,\rm dc}(t) > V_o. \tag{27}$$

With $P_o = 35$ W, $V_o = 48$ V, $\omega = 2\pi \times 50$ rad/s, and $V_{C\,\rm min}$ set at 48 V, the values of $V_{C\,\rm max}$ and $V_{C\,\rm dc}$ can be calculated from (25) and (26) as a function of $C_{\rm dc}$, and be plotted as shown in Fig. 6. It can be seen from the figure that $V_{C\,\rm max}$ increases as $C_{\rm dc}$

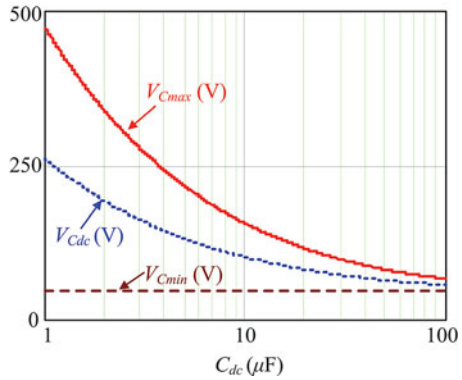

Fig. 6. Plots of $V_{C\max}$, $V_{C\min}$, and $V_{C\,\mathrm{dc}}$ as functions of C_{dc}.

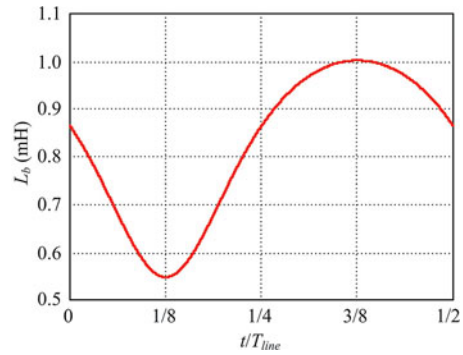

Fig. 7. Plot of the minimum input inductance.

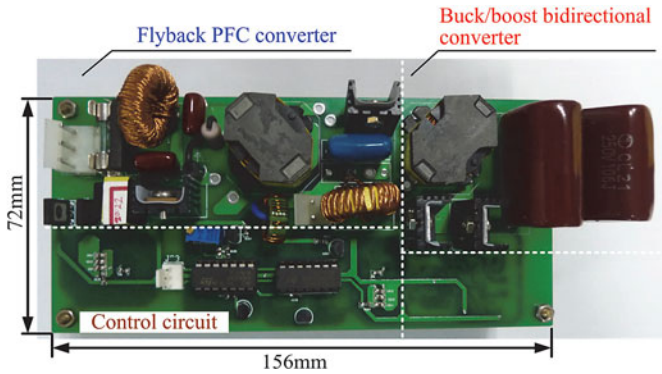

Fig. 8. Photograph of the prototype of the flicker-free electrolytic capacitor-less ac–dc LED driver.

reduces. To have C_{dc} practically realized using film capacitors or ceramic capacitors, its value must be minimized to the extent where there is availability of such components and will lead to an enlargement of the value of $V_{C\max}$. A high $V_{C\max}$ induces a high voltage stress on the two power switches, Q_1 and Q_2, of the bidirectional converter. This forms the lower limit to the permissible value of C_{dc}. Furthermore, note that while C_{dc} is intentionally designed to have a large second-harmonic voltage ripple to reduce its capacitance, the ripple appears only at the output of the bidirectional converter and does not exist in the output voltage V_o of the LED driver.

Here, if C_{dc} is chosen as 20 μF, then from Fig. 6, one can obtain $V_{C\min} = 48$ V, $V_{C\,\mathrm{dc}} = 82$ V, and $V_{C\max} = 115$ V. By setting reference voltage of the controller at $V_{C\,\mathrm{dc\_ref}} = 82$ V, C_{dc} will be regulated at an average voltage of $V_{C\,\mathrm{dc}} = 82$ V and it will contain a voltage ripple with minimum amplitude of $V_{C\min} = 48$ V and maximum amplitude of $V_{C\max} = 115$ V at full load. These are the key parameters representing the worst case operating condition for the design of $C_{\mathrm{dc}} = 20$ μF. Keeping all parameters constant, a higher adopted value of $V_{C\,\mathrm{dc\_ref},}$ which makes $V_{C\min} > 48$ V, $V_{C\,\mathrm{dc}} > 82$ V, and $V_{C\max} > 115$ V, will not affect the proper operation of the converter since $V_{C\min} > V_o = 48$ V. Similarly, a reduction of the output load current, e.g., during dimming, will not affect the proper operation of the converter since $V_{C\min} > V_o = 48$ V, $V_{C\,\mathrm{dc}} = 82$ V, and $V_{C\max} < 115$ V. Finally, a reduction in the output voltage of the driver $V_o < 48$ V (and therefore a reduction in the output power since the current is regulated as a constant), e.g., in the event of an LED failure or when an LED is overheated, will also not affect the proper operation of the proposed converter since $V_{C\min} > 48$ V$> V_o$, $V_{C\,\mathrm{dc}} = 82$ V, and $V_{C\max} < 115$ V. Note that the proper operation of the driver is achieved for all scenarios by setting the $V_{C\,\mathrm{dc\_ref}}$ at a fixed value greater than the value of $V_{C\,\mathrm{dc}}$ given in Fig. 6. There is no requirement for adjusting $V_{C\,\mathrm{dc\_ref}}$ in any situation. In the experimental prototype, $V_{C\,\mathrm{dc\_ref}}$ is set at 110 V, giving $V_{c\mathrm{dc}} = 110$ V, $V_{C\min} = 85$ V, and $V_{C\max} = 136$ V at full load.

B. Buck/Boost Inductor

Two factors must be taken into consideration when choosing the value of the buck/boost inductor L_b. One is to ensure that the inductor current is capable of tracking the current reference, and the other is that the inductor current ripple should be small. The buck/boost inductor should be as small as possible for fast current tracking speed. However, a smaller inductor will result in a larger current ripple. The choice of the inductance is, therefore, a balance between these tradeoffs.

Here, the buck/boost inductor current i_b needs to track the second-harmonic ripple, which is 100 Hz for an ac source with a line frequency of 50 Hz. The switching frequency of the bidirectional converter is chosen as 100 kHz, which is much higher than the 100 Hz. So, in this case, it would be sufficient to choose the value of the buck/boost inductor with sole consideration to the inductor current ripple. The current tracking speed will be proficiently satisfied since the required tracking signal is relatively much slower at 100 Hz. Note that there is no relationship entangling the choice of the switching frequencies of the bidirectional buck/boost converter and the flyback converter. Both are independent of one another.

As the two power switches of the bidirectional converter operate in a complementary manner, the flow of the buck/boost inductor current is bidirectional, which means that the bidirectional converter is operating in continuous current conduction mode. Thus, the relationship of the input and output voltages of the bidirectional converter can be expressed as

$$\frac{v_{C\,\mathrm{dc}}(t)}{V_{Co}} = \frac{1}{1 - d_{Q1}(t)} \tag{28}$$

where $d_{Q\,1}$ is the duty cycle of Q_1.

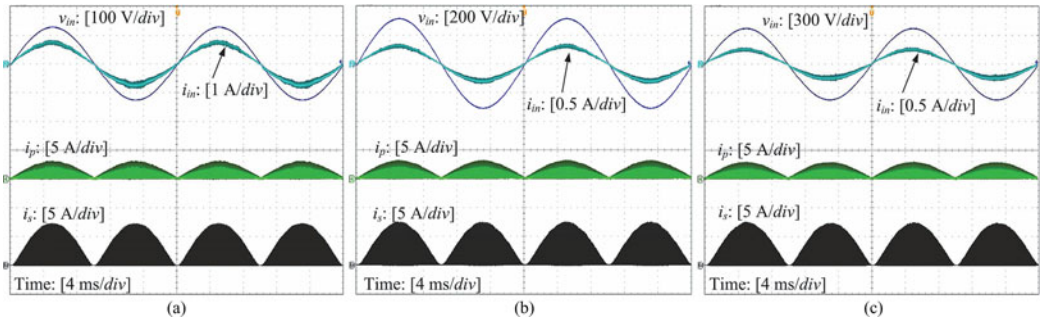

Fig. 9. Waveforms of input voltage, input current, primary current, and secondary current of flyback converter at full load. (a) 90-V input; (b) 220-V input; and (c) 264-V input.

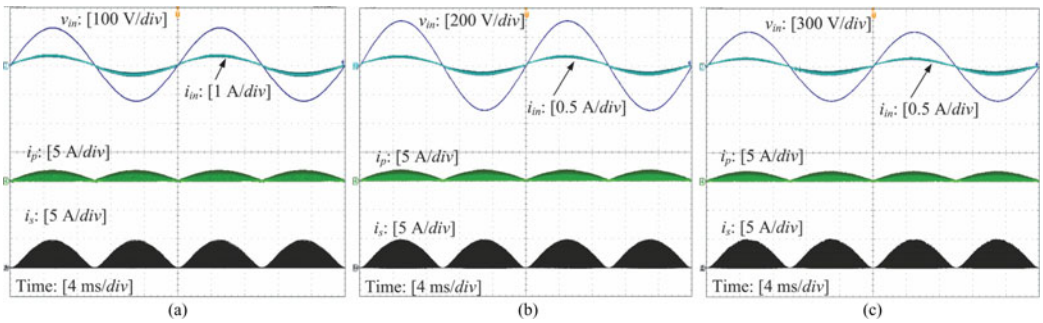

Fig. 10. Waveforms of input voltage, input current, primary and secondary current of flyback converter at half load. (a) 90-V input; (b) 220-V input; and (c) 264-V input.

From (28), we get

$$d_{Q1}(t) = 1 - \frac{V_{Co}}{v_{C\mathrm{dc}}(t)}. \tag{29}$$

When Q_1 is turned ON and Q_2 is turned OFF, the voltage across the buck/boost inductor is V_{Co}. This voltage causes the inductor current to increase. The inductor current ripple can be expressed as

$$\Delta i_L = \frac{V_{Co}}{L_b} d_{Q1}(t) T_{s2} \tag{30}$$

where T_{s2} is the switching period of the power switches Q_1 and Q_2.

The substitution of (29) into (30) gives

$$L_b = \frac{(v_{C\mathrm{dc}}(t) - V_{Co})\, V_{Co} T_{s2}}{v_{C\mathrm{dc}}(t) \Delta i_L}. \tag{31}$$

If we let $\Delta I_{L\_\max} = 0.3$ A and $T_{s2} = 10$ μs, the substitution of (24), $C_{\mathrm{dc}} = 20$ μF, $V_{C\min} = 85$ V, $V_{Co} \approx V_o = 48$ V, and $I_o = 0.7$ A into (31), will generate data that allow us to plot the curve of the minimum buck/boost inductor in a half-line cycle as given in Fig. 7. From the figure, the minimum buck/boost inductor is 0.998 mH. In this study, we choose $L_b = 1.1$ mH.

V. Experimental Verification

In order to verify the validity of the proposed flicker-free electrolytic capacitor-less ac–dc LED driver, a prototype, as shown in Fig. 8, has been built and tested. The specifications of the prototype are as follows: input voltage: $V_{\mathrm{in}} = 90$–264 $\mathrm{V_{AC}}$/50 Hz; output voltage $V_o = 48$ $\mathrm{V_{DC}}$; output current $I_o = 0.7$ A; switching frequency of the flyback converter $f_{s1} = 200$ kHz; switching frequency of the bidirectional converter $f_{s2} = 100$ kHz. The power devices and components of the flyback converter are as follows: turns ratio of the transformer (core is RM10, and the primary and secondary winding are 14 turns and 7 turns, respectively) is $n = 2$; primary inductance $L_p = 80$ μH; filter capacitor $C_o = 0.47$ μF (metalized polyester film capacitor, C212A474 J); filter inductor $L_o = 30$ μH (core is iron powder TN20/13/6, and the winding is 26 turns); power switch Q is FQPF6N60; secondary diode D is RHRP860; and the controller IC is UCC3843. The power devices and components of the bidirectional converter are as follows: $L_b = 1.1$ mH (core is RM10, and the winding is 52 turns); $C_{\mathrm{dc}} = 20$ μF (metalized polyester film capacitor, C212E106J); power switches Q_1 and Q_2 are FQPF2N60; and the controller is made up of UCC3843, CD4011, and IR2110.

Figs. 9 and 10 show the waveforms of the input voltage, input current, primary current, and secondary current of the flyback converter at full load and half load, respectively. As shown in the two figures, for different input voltage and load, the input current is always in phase with the input voltage. Also, the peak values of the primary and secondary currents of the PFC flyback converter are kept relatively constant at different input voltage.

Fig. 11(a) and (b) shows the waveforms of the secondary current i_o', buck/boost inductor current i_b, LED current i_o, and voltage of the capacitor C_{dc} at full load and half load, respectively. It can be seen from both the figures that the second-harmonic ripple in i_o' is absorbed by the bidirectional converter, leaving a relatively pure dc current to drive the LEDs. Thus, the output flux of the LEDs will contain no flicker.

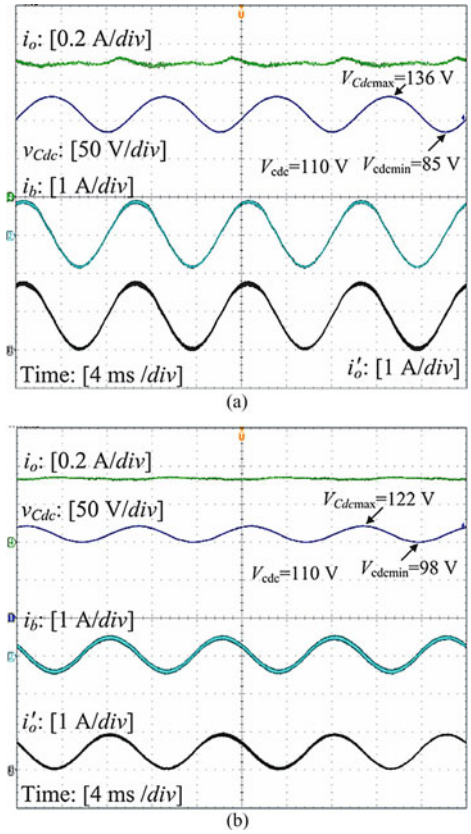

Fig. 11. Waveforms of i'_o, input current, LED current, and filter capacitor voltage. (a) Full load and (b) half load.

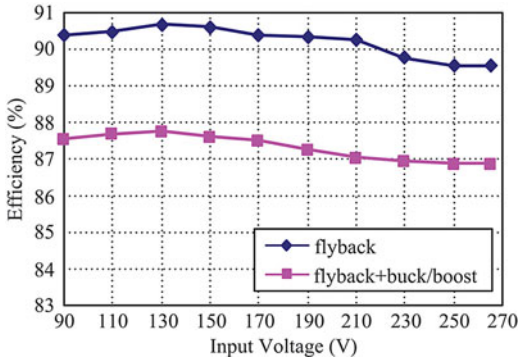

Fig. 12. Efficiency plot of the proposed driver including and excluding the bidirectional buck/boost converter operating at full-load condition for different input voltage.

Fig. 12 shows the efficiency plot of the proposed LED driver with the PFC flyback converter and the bidirectional buck/boost converter operating at full-load condition. The efficiency of the driver averages at around 87% for the entire range of input voltages. Without the bidirectional buck/boost converter, the efficiency of the LED driver averages at around 90%. From this measurement, it can be deduced that the incorporation of the bidirectional buck/boost converter into the LED driver to eliminate light flicker introduces a 3% loss of power.

VI. Conclusion

In order to increase the lifetime of LED drivers to better match the lifetime of LEDs since they exist as an integrated product, the electrolytic capacitor in conventional LED drivers must be removed. The single-stage PFC converter that uses pulsing current to drive LEDs allows the removal of the electrolytic capacitor at the expense of introducing light flicker at twice the power line frequency. A single-phase high power factor flicker-free electrolytic capacitor-less ac–dc LED driver, which consists of a PFC flyback converter and a bidirectional buck/boost converter, has been proposed in this paper. The bidirectional converter buffers the instantaneous power difference between the input and output of the driver, producing only a constant current to drive the LEDs. To greatly reduce the capacitance, so that long-lifetime capacitors such as film capacitor or ceramic capacitor can be used, the capacitor voltage of the bidirectional converter is intentionally designed to have large ripple. As no electrolytic capacitor is required, the proposed LED driver can achieve a longer lifetime than conventionally possible. Concurrently, since the driving current is a pure dc constant current, the problem of flickering is also avoided. The experimental work and results validated the effectiveness of the proposed flicker-free electrolytic capacitor-less ac–dc LED driver.

References

[1] A. Lay-Ekuakille, F. D'Aniello, F. Miduri, D. Leonardi, and A. Trotta, "Smart control of road-based LED fixtures for energy saving," in *Proc. IEEE Intell. Data Acquisition Adv. Comput. Syst.*, 2009, pp. 59–62.

[2] J. Tsao, "Roadmap projects significant LED penetration of lighting market by 2010," *Laser Focus World*, vol. 39, pp. 11–14, May 2003.

[3] J. Sammarco, M. Reyes, J. Bartels, and S. Gallagher, "Evaluation of peripheral visual performance when using incandescent and LED miner cap lamps," *IEEE Trans. Ind. Appl.*, vol. 45, no. 6, pp. 1923–1929, Nov. 2009.

[4] J. Brite, "LED market grew by 93% in 2010, driven by backlights," LEDs Magazine, Feb. 2011.

[5] H. Liu, Y. Yu, and X. Liu, "The research of humanized design of the LED landscape lighting lamp," in *Proc. IEEE Comput.-Aided Ind. Design Conceptual Design*, 2009, pp. 499–502.

[6] D. Yoo and G. Jeong, "LCD panal sector-dimming controlled high efficiency LED backlight drive system," in *Proc. Int. Conf. Electr. Mach. Syst.*, 2009, pp. 1–6.

[7] Y. Lin, J. Zhang, X. Zou, and W. Li, "An efficiency- enhanced low dropout linear HB LED driver for automotive application," in *Proc. IEEE Int. Conf. Electron Devices Solid-State Circuits*, 2008, pp. 1–4.

[8] L. Yin, X. Wu, and M. Zhao, "A highly efficient switched-capacitor LED driver with switching frequency hopping technique," in *Proc. IEEE Solid-State Integr. Circuit Technol.*, 2010, pp. 521–523.

[9] B. Ackerrmann, V. Schulz, C. Martiny, and A. Hilgers, "Control of LEDs," in *Proc. IEEE Ind. Appl. Soc.*, 2006, pp. 2608–2615.

[10] Electromagnetic compatibility, Part 3, Section 2. Limits for harmonic current emissions (equipment input current≤16A per phase), IEC 61000-3-2, 2005.

[11] *Electrolytic Capacitors Application Guide*, Evox Rifa, Espoo, Finland, 2001.

[12] *Lifetime of White LEDs*, Energy Efficiency and Renewable Energy, U.S. Dept. Energy, Washington, DC, Sep. 2009.

[13] L. Han and N. Narendran, "An accelerated test method for predicting the useful life of an LED driver," *IEEE Trans. Power Electron.*, vol. 26, no. 8, pp. 2249–2257, Aug. 2011.

[14] Y. X. Qin, H. S. H. Chung, D. Y. Lin, and S. Y. R. Hui, "Current source ballast for high power lighting emitting diodes without electrolytic capacitor," in *Proc. IEEE Ind. Electron. Soc.*, 2008, pp. 1968–1973.

[15] S. Y. R. Hui, S. N. Li, X. H. Tao, W. Chen, and W. M. Ng, "A novel passive off-line light-emitting diode (LED) driver with long lifetime," in *Proc. IEEE Appl. Power Electron. Conf.*, 2010, pp. 594–600.

[16] I.-H. Oh, "A single-stage power converter for a large screen LCD backlighting," in *Proc. IEEE Appl. Power Electron. Conf.*, 2006, pp. 1058–1063.

[17] J. Shao, "Single stage offline LED driver," in *Proc. IEEE Appl. Power Electron. Conf.*, 2009, pp. 582–586.
[18] L. Gu, X. Ruan, M. Xu, and K. Yao, "Means of eliminating electrolytic capacitor in ac/dc power supplies for LED lighting," *IEEE Trans. Power Electron.*, vol. 24, no. 5, pp. 1399–1408, May 2009.
[19] B. K. Bose and D. Kastha, "Electrolytic capacitor elimination in power electronic system by high frequency active filter," in *Proc. IEEE Ind. Appl. Soc.*, 1991, pp. 869–78.
[20] C. Y. Hsu and H. Y. Wu, "A new single-phase active power filter with reduced energy-storage capacity," *IEE Proc. Electric Power Appl.*, vol. 143, no. 1, pp. 25–30, Jan. 1996.
[21] A. C. Kyritsis, N. P. Papanikolaou, and E. C. Tatakis, "A novel parallel active filter for current pulsation smoothing on single stage grid-connected ac-PV modules," in *Proc. Eur. Conf. Power Electron. Appl.*, 2007, pp. 1–10.
[22] P. T. Krein and R. S. Balog, "Cost-effective hundred-year life for single-phase inverter and rectifiers in solar and LED lighting applications based on minimum capacitance requirements and a ripple power port," in *Proc. IEEE Appl. Power Electron. Conf.*, 2009, pp. 620–625.
[23] R. Wang, F. Wang, D. Boroyevich, and P. Ning, "A high power density single phase PWM rectifier with active ripple energy storage," in *Proc. IEEE Appl. Power Electron. Conf.*, 2010, pp. 1378–1383.
[24] G. Spiazzi, S. Buso, and G. Meneghesso, "Analysis of a high-power-factor electronics ballast for high brightness lighting emitting diodes," in *Proc. IEEE Power Electron. Spec. Conf.*, 2005, pp. 1494–1499.
[25] B. Wang, X. Ruan, M. Xu, and K. Yao, "A method of reducing the peak-to-average ratio of LED current for electrolytic capacitor-less ac/dc drivers," *IEEE Trans. Power Electron.*, vol. 25, no. 3, pp. 592–601, Mar. 2010.
[26] L. Peretto, E. Pivello, R. Tinarelli, and A. E. Emanuel, "Theoretical analysis of the physiologic mechanism of luminous variation in eye–brain system," *IEEE Trans. Instrum. Meas.*, vol. 56, no. 1, pp. 164–170, Feb. 2007.
[27] K. Taekhyun, M. Rylander, E. Powers, W. Grady, and A. Arapostathis, "LED lamp flicker caused by interharmonics," in *Proc. IEEE Int. Instrum. Meas. Technol. Conf.*, 2008, pp. 1920–1925.
[28] A. Wilkins, J. Veitch, and B. Lehman, "LED lighting flicker and potential health concerns IEEE standard PAR1789 update," in *Proc. IEEE Energy Convers. Congr. Expo.*, 2010, pp. 171–178.

Shu Wang was born in Jiangsu Province, China, in 1985. He received the B.S. and M.S. degrees in electrical engineering from the Nanjing University of Aeronautics and Astronautics, Nanjing, China, in 2008 and 2011, respectively.

Since March 2011, he has been with the Clean Energy Research Institute, State Grid Electric Power Research Institute, Nanjing. His main research interests include dc–dc converters, ac–dc converters, and power supplies for LED.

Xinbo Ruan (M'97–SM'02) was born in Hubei Province, China, in 1970. He received the B.S. and Ph.D. degrees in electrical engineering from the Nanjing University of Aeronautics and Astronautics (NUAA), Nanjing, China, in 1991 and 1996, respectively.

In 1996, he joined the Faculty of Electrical Engineering Teaching and Research Division, NUAA, where he became a Professor in 2002 in the College of Automation Engineering, NUAA, and has been involved in teaching and research in the field of power electronics. From August to October 2007, he was a Research Fellow in the Department of Electronics and Information Engineering, Hong Kong Polytechnic University, Hong Kong. He has also been the College of Electrical and Electronic Engineering, Huazhong University of Science and Technology, Wuhan, China, since March 2008. He is a Guest Professor at Beijing Jiaotong University, Beijing, China, the Hefei University of Technology, Hefei, China, and Wuhan University, Wuhan. He is the author or coauthor of three books and more than 130 technical papers published in journals and conferences. His main research interests include soft-switching dc/dc converters, soft-switching inverters, power factor correction converters, modeling the converters, power electronics system integration, and renewable energy generation system.

Dr. Ruan was awarded the Delta Scholar by the Delta Environment and Education Fund in 2003, and was awarded the Special Appointed Professor of the Chang Jiang Scholars Program, by the Ministry of Education, China, in 2007. In 2005, he has served as the Vice President of the China Power Supply Society, and since 2008, he has been a member of the Technical Committee on Renewable Energy Systems within the IEEE Industrial Electronics Society. He has also been an Associate Editor for the IEEE TRANSACTIONS ON INDUSTRIAL ELECTRONICS since 2011. He is a Senior Member of the IEEE Power Electronics Society and the IEEE Industrial Electronics Society.

Kai Yao was born in Jiangsu Province, China, in 1980. He received the B.S. degree in industrial automation from Nantong University, Nantong, China, in 2002, the M.S. degree in mechanical design and theory and the Ph.D. degree in electrical engineering from the Nanjing University of Aeronautics and Astronautics, Nanjing, China, in 2005 and 2010, respectively.

Since April 2011, he has been with the College of Automation Engineering, Nanjing University of Science and Technology, Nanjing. His main research interests include dc/dc converters, ac/dc converters, and power supplies for LED.

Siew-Chong Tan (S'00–M'06–SM'11) received the B.Eng. (Hons.) and M.Eng. degrees in electrical and computer engineering from the National University of Singapore, Singapore, in 2000 and 2002, respectively, and the Ph.D. degree in electronic and information engineering from the Hong Kong Polytechnic University, Kowloon, Hong Kong, in 2005.

He is currently an Assistant Professor in Department of Electronic and Information Engineering, Hong Kong Polytechnic University. His current research interests include nonlinear control of power electronic systems, switched-capacitor converter circuits and applications, and the development of power-electronic-based circuits for light-emitting diodes. He serves extensively as a Reviewer for various IEEE/IET transactions and journals on power, electronics, circuits, and control engineering. He is the coauthor of *Sliding Mode Control of Switching Power Converters: Techniques and Implementation* (Boca Raton, FL: CRC Press, 2011).

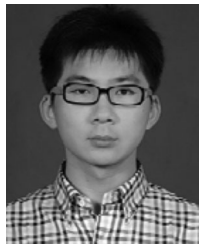

Yang Yang was born in Shaanxi Province, China, in 1988. He received the B.S. degree in electrical engineering and automatization from the Nanjing University of Aeronautics and Astronautics, Nanjing, China, in 2010, where he is currently working toward the M.S. degree in electrical engineering.

His main research interests include ac/dc converters and power supplies for LED.

Zhihong Ye was born in Zhejiang Province, China, in 1969. He received B.S. and M.S. degrees in electrical engineering from Tsinghua University, Beijing, China, in 1992 and 1994, respectively, and the Ph.D. degree from the Bradley Department of Electrical and Computing Engineering, Virginia Polytechnic Institute and State University, Blacksburg, in 2000.

From 2000 to 2005, he was an Electrical Engineer at General Electric Global Research Center, Niskayuna, NY. From 2005 to 2006, he was with Dell as a Commodity Quality Manager. Since 2006, he has been with Lite-On Technology Corp., Nanjing, China, as the Director of Research and Development. He holds seven U.S. patents, and has published more than 30 technical papers in transactions and international conferences. His research interests include high density, high-efficiency power supply for computing, communication, and consumer electronics applications, digital control, power converter topologies and controls, soft-switching techniques, etc.